

The American Journal of Sports Medicine

<http://ajs.sagepub.com/>

Radiographic Identification of the Primary Lateral Ankle Structures

C. Thomas Haytmanek, Brady T. Williams, Evan W. James, Kevin J. Campbell, Coen A. Wijdicks, Robert F. LaPrade
and Thomas O. Clanton

Am J Sports Med 2015 43: 79 originally published online October 16, 2014

DOI: 10.1177/0363546514553778

The online version of this article can be found at:

<http://ajs.sagepub.com/content/43/1/79>

Published by:



<http://www.sagepublications.com>

On behalf of:

American Orthopaedic Society for Sports Medicine



Additional services and information for *The American Journal of Sports Medicine* can be found at:

Email Alerts: <http://ajs.sagepub.com/cgi/alerts>

Subscriptions: <http://ajs.sagepub.com/subscriptions>

Reprints: <http://www.sagepub.com/journalsReprints.nav>

Permissions: <http://www.sagepub.com/journalsPermissions.nav>

>> [Version of Record](#) - Dec 31, 2014

[OnlineFirst Version of Record](#) - Oct 16, 2014

[What is This?](#)

Radiographic Identification of the Primary Lateral Ankle Structures

C. Thomas Haytmanek,^{*†} MD, Brady T. Williams,^{*} BS, Evan W. James,^{*} BS, Kevin J. Campbell,^{*} MD, Coen A. Wijdicks,^{*} PhD, Robert F. LaPrade,^{*†} MD, PhD, and Thomas O. Clanton,^{*†‡} MD

Investigation performed at the Department of BioMedical Engineering, Steadman Philippon Research Institute, Vail, Colorado, USA

Background: Lateral ankle ligament injuries rank among the most frequently observed athletic injuries, requiring repair or reconstruction when indicated. However, there is a lack of quantitative data detailing the ligament attachment sites on standard radiographic views.

Purpose: To quantitatively describe the anatomic attachment sites of the anterior talofibular ligament (ATFL), calcaneofibular ligament (CFL), and posterior talofibular ligament (PTFL) on standard radiographic views with respect to reproducible osseous landmarks to assist with intraoperative and postoperative assessment of lateral ankle ligament repairs and reconstructions.

Study Design: Descriptive laboratory study.

Methods: Twelve nonpaired, fresh-frozen cadaveric foot and ankle specimens were dissected to identify the origins and insertions of the 3 primary lateral ankle ligaments. Ligament footprint centers were marked with 2-mm stainless steel spheres shallowly embedded at the level of the cortical bone prior to obtaining standard lateral and mortise radiographs. Measurements were performed twice by 2 blinded raters independently to calculate mean distances and assess reliability via intraclass correlation coefficients (ICCs).

Results: Radiographic measurements demonstrated excellent reproducibility between raters (all interobserver ICCs > 0.97) and across trials (all intraobserver ICCs > 0.99). On the lateral view, the ATFL fibular attachment (mean \pm SD) was 8.4 ± 1.8 mm proximal and anterior to the inferior tip of the lateral malleolus and attached on the talus 13.8 ± 2.0 mm proximal and anterior to the apex of the lateral talar process. The CFL originated 5.0 ± 1.4 mm superior and anterior to the inferior tip of the lateral malleolus and inserted on the calcaneus 18.5 ± 4.6 mm posterior and superior to the posterior point of the peroneal tubercle. On the mortise view, the ATFL origin was 4.9 ± 1.4 mm proximal to the inferior tip of the lateral malleolus and inserted on the talus 9.0 ± 2.1 mm medial and superior of the apex of the lateral talar process and 18.9 ± 3.1 mm inferior and slightly lateral to the superior lateral corner of the talar dome. The fibular CFL origin was 2.9 ± 1.6 mm proximal and slightly medial to the inferior tip of the lateral malleolus and inserted on the calcaneus 18.0 ± 5.1 mm distal to the apex of the lateral talar process.

Conclusion: Radiographic parameters quantitatively describing the anatomic origins and insertions of the lateral ankle ligaments were defined with excellent reproducibility and agreement between reviewers.

Clinical Relevance: Quantitative radiographic anatomy data will assist in preoperative planning, improve intraoperative localization, and provide objective measures for postoperative assessment of anatomic repairs and reconstructions.

Keywords: anterior talofibular ligament; calcaneofibular ligament; posterior talofibular ligament; lateral ankle ligament reconstruction; lateral ankle instability; radiographic landmarks

[‡]Address correspondence to Thomas O. Clanton, MD, Steadman Philippon Research Institute, 181 West Meadow Drive, Suite 1000, Vail, CO 81657, USA (e-mail: tclanton@thesteadmanclinic.com).

^{*}Steadman Philippon Research Institute, Vail, Colorado, USA.

[†]The Steadman Clinic, Vail, Colorado, USA.

One or more of the authors has declared the following potential conflict of interest or source of funding: R.F.L. is a paid consultant for Arthrex Inc and receives research support from Arthrex, Smith & Nephew, Ossur, and Linvatec. T.O.C. is a paid consultant for Arthrex Inc and Stryker and serves on lectures on speakers bureaus for Arthrex, SBI, Smith & Nephew, and Stryker.

Lateral ankle sprains are defined as injury to any of the 3 primary ligaments of the lateral ligament complex, which includes the anterior talofibular ligament (ATFL), the calcaneofibular ligament (CFL), and the posterior talofibular ligament (PTFL). Lateral ankle sprains are estimated to account for as much as 85% of ankle sprains and 15% to 20% of all athletic injuries.^{7,12,21,28} The incidence of ankle sprains in the 15- to 19-year age group is 7.2 per 1000 person-years in the United States, making this a significant clinical concern.³¹

Most lateral ankle sprains are low-grade injuries and can be treated nonoperatively. However, historically up to 20% of these patients experience chronic instability

that may require surgical intervention to restore lateral ankle stability.^{14,15,20} In such instances, both anatomic and nonanatomic surgical methods exist. Regardless of surgical treatment, a thorough knowledge of lateral ankle anatomy is necessary to ensure a successful outcome. Previous anatomical studies have both qualitatively and quantitatively defined structures of the lateral ankle to advance repair and reconstruction techniques based on anatomic principles.⁸ While anatomic studies are numerous, the current literature has presented minimal data that sufficiently characterize lateral ankle anatomy with respect to radiographic landmarks.²⁷ Such information could be used to improve preoperative planning, augment intraoperative visualization, and assist in postoperative assessment of anatomic repairs and reconstructions. Quantitative radiographic anatomy would be of particular use in revision cases where ligament and other soft tissue anatomy may be obscured by scarring and previous surgical repairs or in arthroscopically assisted cases in which anatomic landmarks typically used during open repairs or reconstructions may be poorly visualized.

Therefore, the purpose of this study was to establish quantitative descriptions of radiographic landmarks for the origins and insertions of the 3 main lateral ankle ligaments. We hypothesized that the ligament attachment sites could be reproducibly defined on radiographic images with respect to anatomic osseous landmarks and superimposed radiographic reference lines.

MATERIALS AND METHODS

Specimen Preparation

Twelve nonpaired, fresh-frozen cadaveric specimens with an average age of 58.9 years (range, 50-82 years; 10 male, 2 female) with no previous history of ankle injury, osteoarthritis, or osteophytes were used in this study. Tibial and fibular neutral orientations were fixed with 2 transverse rigid screws placed approximately 10 and 15 cm proximal to the tibial plafond to mimic the native anatomic relationships that would otherwise be stabilized proximally by the ligamentous and bony structures of the proximal tibiofibular joint. Dissections excised all overlying adipose, muscular, tendinous, and neurovascular tissue to expose the ligamentous structures and their attachment sites at the lateral ankle. After gross anatomic dissections were completed, 1 male specimen was excluded because of significant osteophyte formation along the tibiotalar joint line, leaving a total of 11 specimens (9 male, 2 female) for inclusion in this study (mean height and foot length [\pm SD] of 174.1 \pm 8.1 cm and 24.8 \pm 1.8 cm, respectively).

The 3 lateral ligaments and their respective proximal and distal footprints were identified. A longitudinal incision was made along the axis of each ligament by splitting the ligament fibers lengthwise down to the level of cortical bone at the center of each site of attachment. This incision allowed the center of each footprint to be accessed and



Figure 1. A modified anatomic illustration from Clanton et al⁴ of the lateral ankle. A graphical representation of the anterior talofibular ligament (ATFL) origin (1) and insertion (2) and calcaneofibular ligament (CFL) origin (3) and insertion (4) that have been marked with 2-mm stainless steel spheres. A subset of selected anatomic osseous landmarks used for radiographic reference measurements is also indicated (arrows): a, distal point of the talar neck; b, proximal point of the talar neck; c, anterior fibular tubercle; d, apex of the lateral talar process; e, inferior tip of the lateral malleolus; f, posterior point of the peroneal tubercle; and i, posterior point of the calcaneus.

marked with a 2-mm-diameter stainless steel sphere (diameter, 2.0 \pm 0.0025 mm; sphericity, 0.0006; Small Parts Inc) superficially implanted in the cortical bone using a previously described technique (Figures 1 and 2).^{11,22,23,32} In the case of the ATFL, where several specimens exhibited a ligament composed of 2 distinct bands,⁴ the 2-mm stainless steel sphere was placed at the midpoint between the 2 footprint centers. In addition, the posterior point of the peroneal tubercle was marked with a 2-mm stainless steel sphere.

Data Collection

A miniature fluoroscopy C-arm (Hologic Inc) was used to obtain standard lateral and mortise radiographs for each specimen. True lateral and mortise radiographic views were obtained in accordance with established standard definitions.¹⁸ Lateral radiographs were defined as superimposition of the lateral and medial malleoli and aspects of the talar dome (Figure 2). Mortise view images were taken with approximately 15° of internal rotation to confer a single horizontal plane containing both medial and lateral malleoli (Figure 2). A 25.4-mm-diameter stainless steel sphere (diameter, 25.4 \pm 0.00254 mm; sphericity, 0.00061 mm; Small Parts Inc) was included directly in the plane

⁸References 1, 2, 4, 5, 9, 17, 20, 24, 27, 28, 33.

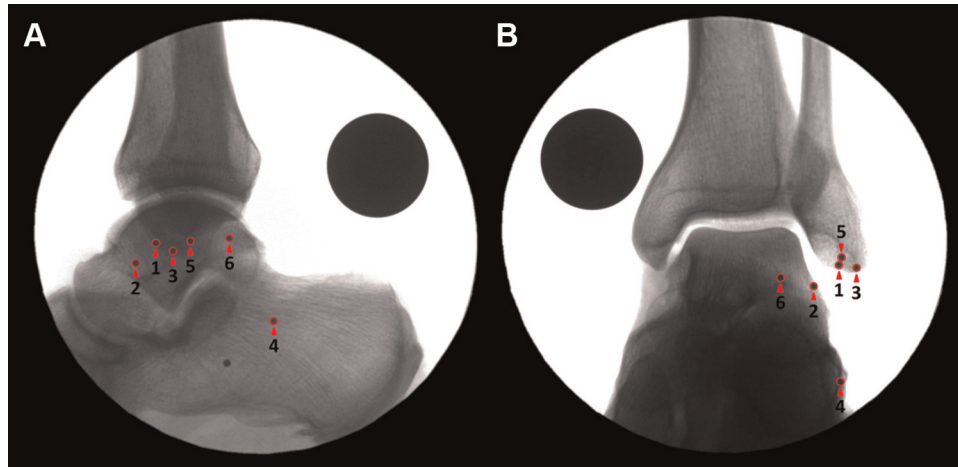


Figure 2. True (A) lateral and (B) mortise radiographs identifying the attachment sites of the anterior talofibular ligament (ATFL; 1, fibular attachment; 2, talar attachment), the calcaneofibular ligament (CFL; 3, fibular attachment; 4, calcaneal attachment), and the posterior talofibular ligament (PTFL; 5, fibular attachment; 6, talar attachment).

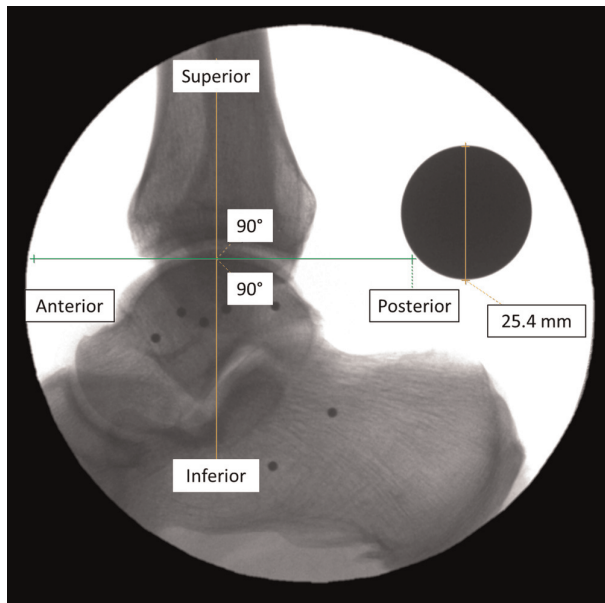


Figure 3. Lateral radiograph demonstrating the measurement reference frame and axes established for radiographic measurements.

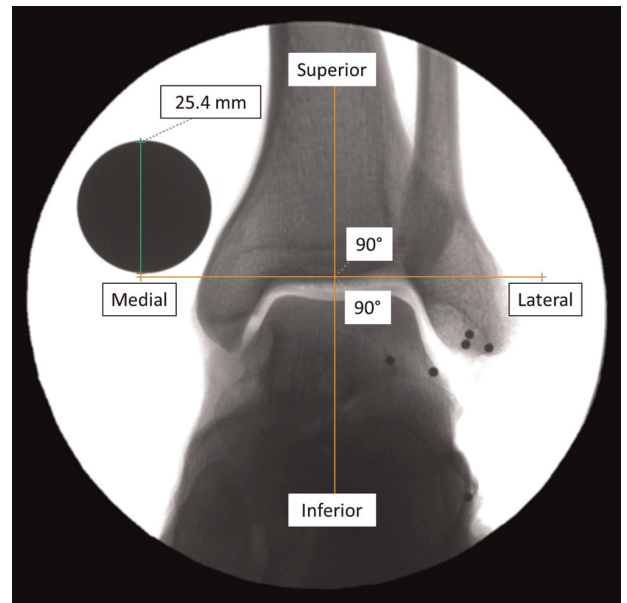


Figure 4. Mortise radiograph demonstrating the measurement reference frame and axes established for radiographic measurements.

of the specimen using a custom fixture to account for any fluctuation in magnification due to varying specimen distance from the x-ray source and for measurement calibration. The 25.4-mm sphere was positioned in the imaging field using a custom adjustable-height fixture set at the level of the lateral ankle ligaments.

Measurements

Radiographic images were uploaded and calibrated in a picture archiving and communication system (PACS) (eFilm Workstation 3.4; Merge Healthcare Inc). Images were

calibrated using the 25.4-mm stainless steel sphere positioned in the radiographic field of view. Measurements describing the spatial relationships between ligament sites of attachment and surgically relevant osseous landmarks were collected in a spreadsheet (Microsoft Corp).

For lateral radiographs, the anterior-posterior axis was established by a horizontal line drawn through the distal margins of the anterior and posterior tibial plafond (Figure 3). The inferior-superior axis was established by creating a line perpendicular to the anterior-posterior axis line. For the directionality components, measurements made in the anterior and superior directions were assigned

TABLE 1
Radiographic Measurements of the Lateral Ankle Ligaments, Lateral View^a

	Absolute Distance, mm, Mean ± SD	Directionality, mm, Mean	
		Anterior (+)/ Posterior (-)	Superior (+)/ Inferior (-)
Anterior talofibular ligament			
Distance between attachments (fibula → talus)	9.4 ± 2.4	8.7	-2.3
Talar attachment to proximal point of the talar neck	12.9 ± 3.7	9.7	7.8
Talar attachment to distal point of the talar neck (talonavicular joint line)	25.8 ± 3.8	24.8	4.9
Talar attachment to apex of the lateral talar process	13.8 ± 2.0	-6.0	-12.0
Fibular attachment to CFL fibular attachment	5.8 ± 1.8	-5.0	-1.1
Fibular attachment to PTFL fibular attachment	8.6 ± 1.2	-8.2	1.1
Fibular attachment to inferior tip of the lateral malleolus	8.4 ± 1.8	-5.6	-5.9
Fibular attachment to anterior fibular tubercle	16.9 ± 3.1	9.3	13.8
Calcaneofibular ligament			
Distance between attachments (fibula → calcaneus)	28.1 ± 4.8	-17.1	-15.7
Calcaneal attachment to posterior point of the peroneal tubercle	18.5 ± 4.6	17.0	-5.9
Calcaneal attachment to calcaneal apex	18.6 ± 3.4	7.0	16.8
Calcaneal attachment to posterior point of the calcaneus	22.1 ± 2.0	-20.4	6.6
Fibular attachment to PTFL fibular attachment	4.5 ± 2.1	-3.2	2.5
Fibular attachment to inferior tip of the lateral malleolus	5.0 ± 1.4	-0.5	-4.5
Fibular attachment to anterior fibular tubercle	21.1 ± 3.1	14.3	15.1
Posterior talofibular ligament			
Distance between attachments (fibula → talus)	10.5 ± 2.0	-9.6	0.7
Talar attachment to posterolateral talar tubercle	6.8 ± 3.2	-5.5	-3.4
Fibular attachment to inferior tip of the lateral malleolus	7.9 ± 2.5	2.8	-7.0
Fibular attachment to anterior fibular tubercle	21.8 ± 3.0	17.2	13.0

^aCFL, calcaneofibular ligament; PTFL, posterior talofibular ligament.

TABLE 2
Interobserver Reliability^a

Interobserver	Mortise			Lateral		
	ICC	LB	UB	ICC	LB	UB
ATFL	0.986	0.979	0.991	0.984	0.975	0.989
PTFL	0.986	0.977	0.992	0.984	0.971	0.991
CFL	0.99	0.985	0.994	0.975	0.961	0.984

^aATFL, anterior talofibular ligament; CFL, calcaneofibular ligament; ICC, intraclass correlation coefficient; LB, lower bound; PTFL, posterior talofibular ligament; UB, upper bound.

positive values. Measurements made in the posterior and inferior directions were assigned negative values.

For mortise radiographs, the medial-lateral axis was established by a horizontal line drawn parallel to the tibial plafond (Figure 4). The inferior-superior axis was established by creating a line perpendicular to the medial-lateral axis. Measurements made in the lateral and superior directions were assigned positive values, while measurements made in the medial and inferior directions were assigned negative values.

Radiographic landmarks were described and defined by the senior author (T.O.C.) and an orthopaedic foot and ankle fellow (C.T.H.) and can be appreciated in Figures 1, 5, and 6. Distances were recorded to the most extreme extent of each particular structure. For example, the

TABLE 3
Intraobserver Reproducibility^a

Intraobserver	Mortise			Lateral		
	ICC	LB	UB	ICC	LB	UB
ATFL	0.992	0.988	0.995	0.992	0.988	0.995
PTFL	0.993	0.988	0.996	0.991	0.984	0.995
CFL	0.995	0.991	0.997	0.997	0.995	0.998

^aATFL, anterior talofibular ligament; CFL, calcaneofibular ligament; ICC, intraclass correlation coefficient; LB, lower bound; PTFL, posterior talofibular ligament; UB, upper bound.

inferior tip of the lateral malleolus was defined as the most distal point of the fibula in accordance with established axes. Likewise, the anterior fibular tubercle was defined by the most anterior point, and measurements to the apex of the lateral talar process used the most distal point.

Using these frames of reference, all measurements reported in this study were collected using 3 components: the absolute distance between 2 points, the anterior-posterior (lateral view) or medial-lateral (mortise view) directionality component, and the superior-inferior directionality component. All measurements were performed in a blinded fashion by 2 independent reviewers (E.W.J. and B.T.W.) with varying degrees of medical training (1 medical student and 1 pre-medical student) under the direct instruction of an

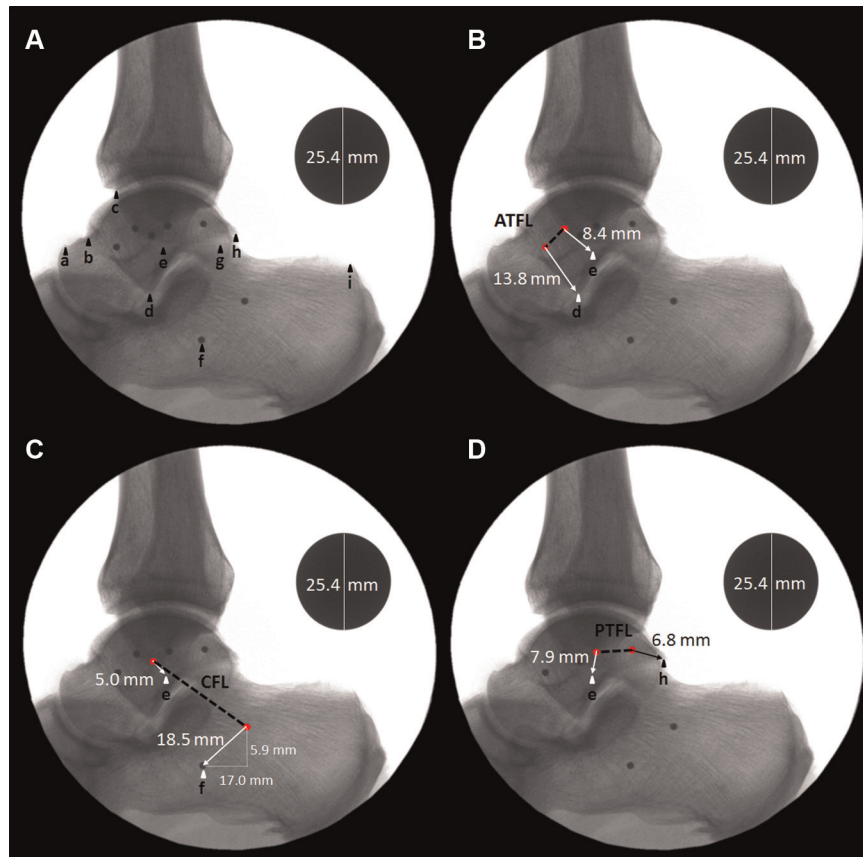


Figure 5. (A) Labeled radiographic landmarks for the lateral view: a, distal point of the talar neck; b, proximal point of the talar neck; c, anterior fibular tubercle; d, apex of the lateral talar process; e, inferior tip of the lateral malleolus; f, posterior point of the peroneal tubercle; g, calcaneal apex; h, posterolateral talar tubercle; i, posterior point of the calcaneus. (B-D) Labeled subset of surgically relevant landmarks for the (B) anterior talofibular ligament (ATFL), (C) calcaneofibular ligament (CFL), and (D) posterior talofibular ligament (PTFL). Distances are reported as means and are diagrammed on a representative lateral radiographic view.

orthopaedic foot and ankle fellow (C.T.H.) and the senior author (T.O.C.; foot and ankle fellowship-trained and 32 years of experience). Each reviewer performed measurements on 2 separate occasions at least 2 weeks apart to allow for the calculation of intraclass correlation coefficients (ICCs) with minimal recall bias.

Statistical Analysis

Distances between sites of ligament attachments were reported as means and standard deviations for each absolute distance measurement using the values of the primary reviewer's (B.T.W.) first set of measurements. Directionality, as determined by the established axes, was averaged and used to report the components of directionality for each measurement. Statistical analyses were performed using SPSS Statistics, version 20 (SPSS Inc, an IBM Company) to calculate 2-way mixed, random measure ICCs for each ligament and radiographic view.²⁶ Interobserver reliability was evaluated using the first set of measurements for both reviewers as a measure of agreement across reviewers. Intraobserver reproducibility was evaluated using the first and second sets of recorded measurements for the primary reviewer.²⁶

RESULTS

Lateral Radiographic View

Select radiographic measurements for the lateral view are reported for each ligament attachment site in Table 1 as means and standard deviations. These relationships are demonstrated in Figure 5. Interobserver and intraobserver ICCs demonstrated excellent agreement and reproducibility, as reported for each ligament in Tables 2 and 3.

On the lateral view radiograph, the ATFL measured 9.4 ± 2.4 mm between insertion sites originating 8.4 ± 1.8 mm proximal to the inferior tip of the lateral malleolus on the anterior aspect of the fibula. This equated to $35.7\% \pm 8.9\%$ of the absolute distance between the inferior tip of the lateral malleolus and the anterior fibular tubercle. The talar insertion of the ligament was 13.8 ± 2.0 mm proximal and anterior to the apex of the lateral process of the talus, measured along the border of the lateral process, which was approximately $56.2\% \pm 10.1\%$ of the absolute distance between the apex of the lateral process and the proximal origin of the talar neck.

TABLE 4
Radiographic Measurements of the Lateral Ankle Ligaments, Mortise View^a

	Absolute Distance, mm, mean \pm SD	Directionality, mm, Mean	
		Lateral (+)/ Medial (-)	Superior (+)/ Inferior (-)
Anterior talofibular ligament			
Distance between attachments (fibula \rightarrow talus)	12.6 \pm 1.8	-12.3	0.1
Talar attachment to CFL calcaneal attachment	23.7 \pm 3.8	4.1	-22.8
Talar attachment to PTFL talar attachment	8.5 \pm 2.4	-7.4	-0.6
Talar attachment to apex of the lateral talar process	9.0 \pm 2.1	6.3	-6.2
Talar attachment to superior lateral corner of the talar dome	18.9 \pm 3.1	-1.9	18.6
Talar attachment to subtalar joint line	5.2 \pm 1.9	0.0	-5.2
Fibular attachment to CFL fibular attachment	3.9 \pm 1.2	1.5	-1.4
Fibular attachment to PTFL fibular attachment	3.1 \pm 1.5	-1.0	0.9
Fibular attachment to inferior tip of the lateral malleolus	4.9 \pm 1.4	2.1	-4.0
Calcaneofibular ligament			
Distance between attachments (fibula \rightarrow calcaneus)	24.5 \pm 4.5	-9.5	-22.2
Calcaneal attachment to PTFL talar attachment	25.4 \pm 3.3	-11.5	22.2
Calcaneal attachment to apex of the lateral talar process	18.0 \pm 5.1	2.0	17.5
Calcaneal attachment to superior lateral corner of the talar dome	42.3 \pm 5.5	-6.0	41.5
Calcaneal attachment to subtalar joint line	15.3 \pm 4.2	-1.2	15.1
Fibular attachment to PTFL fibular attachment	5.6 \pm 3.5	-1.3	3.4
Fibular attachment to inferior tip of the lateral malleolus	2.9 \pm 1.6	0.8	-2.1
Posterior talofibular ligament			
Distance between attachments (fibula \rightarrow talus)	19.5 \pm 2.5	-17.8	-2.9
Talar attachment to apex of the lateral talar process	15.2 \pm 2.1	13.8	-5.1
Talar attachment to superior lateral corner of the talar dome	20.2 \pm 3.3	5.1	17.2
Talar attachment to subtalar joint line	3.8 \pm 1.4	0.0	-3.8
Fibular attachment to inferior tip of the lateral malleolus	6.1 \pm 1.0	3.3	-4.6

^aCFL, calcaneofibular ligament; PTFL, posterior talofibular ligament.

The CFL measured 28.1 ± 4.8 mm between insertion sites. The CFL originated on the fibula 5.0 ± 1.4 mm superior and anterior to the inferior tip of the lateral malleolus, which was $21.1\% \pm 6.4\%$ of the absolute distance between the inferior tip of the lateral malleolus and the anterior fibular tubercle. The CFL inserted 18.5 ± 4.6 mm posterior and superior (17.0 mm posterior, 5.9 mm superior) to the peroneal tubercle.

The PTFL spanned an interinsertional distance of 10.5 ± 2.0 mm. The fibular origin was 7.9 ± 2.5 mm superior and posterior to the inferior tip of the lateral malleolus. The PTFL insertion was 6.8 ± 3.2 mm anterior and superior to the posterolateral talar tubercle.

Mortise Radiographic View

Select radiographic measurements for the mortise view are reported for each ligament attachment site in Table 4 as means and standard deviations and can be observed in Figure 6. Interobserver and intraobserver ICCs demonstrated excellent agreement and reproducibility, as reported for each ligament in Tables 2 and 3.

On the mortise view, the ATFL interinsertional distance spanned 12.6 ± 1.8 mm. The fibular ATFL attachment was 4.9 ± 1.4 mm proximal and medial to the inferior tip of the lateral malleolus. The ATFL inserted on the talus 9.0 ± 2.1 mm medial and superior to the apex of the lateral talar

process and 18.9 ± 3.1 mm inferior and slightly lateral to the superior lateral corner of the talar dome.

The CFL coursed inferior and medial 24.5 ± 4.5 mm between insertions sites on the mortise view. The center of the fibular CFL footprint was 2.9 ± 1.6 mm proximal and slightly medial to the inferior tip of the lateral malleolus and inserted on the calcaneus 18.0 ± 5.1 mm distal to the apex of the lateral talar process.

The PTFL coursed 19.5 ± 2.5 mm between its origin and insertion. The PTFL originated 6.1 ± 1.0 mm proximal and medial to the inferior tip of the lateral malleolus and inserted on the talus 15.2 ± 2.1 mm medial and superior to the apex of the lateral talar process.

DISCUSSION

The most important findings of this study were that reproducible measurements of lateral ankle ligament attachment sites with respect to surgically relevant radiographic landmarks were determined on lateral and mortise radiographs with excellent intra- and interobserver agreement. These findings are of immediate clinical relevance because they provide intraoperative radiographic guidelines for anatomic placement of both lateral ligament repair anchors and reconstruction tunnels. Furthermore, this information is particularly useful in

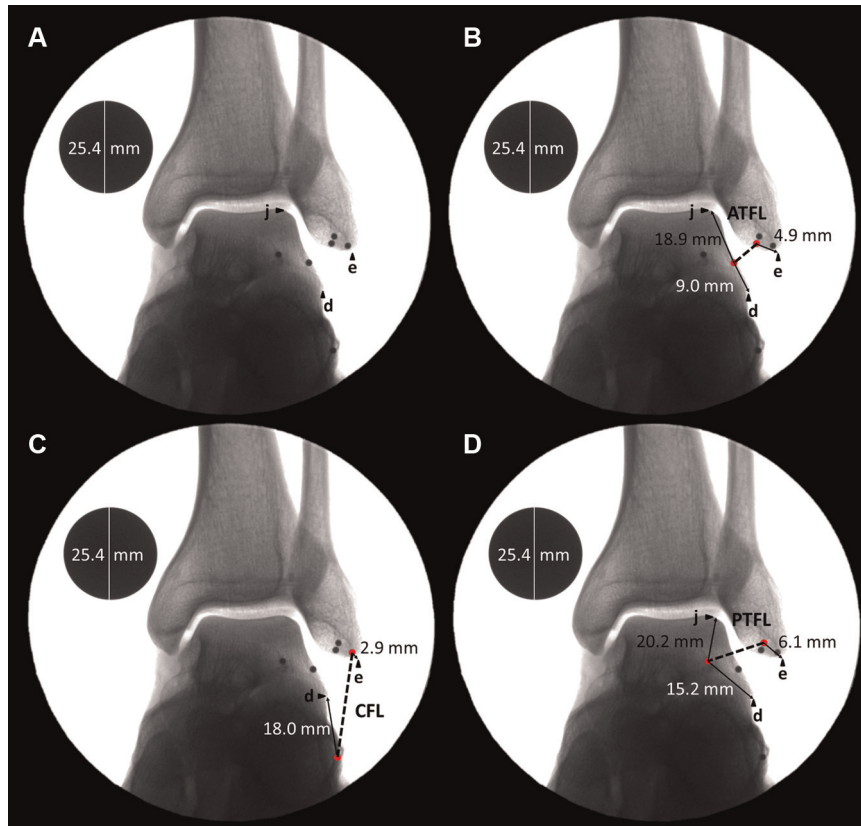


Figure 6. (A) Labeled radiographic landmarks for the mortise view: j, superior lateral corner of the talar dome; d, apex of the lateral talar process; e, inferior tip of the lateral malleolus. (B-D) Labeled subset of surgically relevant landmarks for the (B) anterior talofibular ligament (ATFL), (C) calcaneofibular ligament (CFL), and (D) posterior talofibular ligament (PTFL). Distances are reported as means and are diagrammed on a representative mortise radiographic view.

revision cases, where scarring or prior nonanatomic repairs may obscure the native positions of the ligaments.

Successful anatomic lateral ankle repair or reconstruction is predicated on a comprehensive understanding of lateral ankle anatomy. Currently, radiographic parameters for guiding lateral ankle repair and reconstruction are limited. Taser et al²⁷ evaluated the lateral ligaments of the ankle by dissecting the ligaments and covering them with radiopaque material. This study defined angles and distances to attachments via gross anatomic reference points rather than radiographic landmarks. The current study expands on such data by quantitatively describing the attachment sites with respect to radiographic landmarks for each of the 3 lateral ankle ligaments. The radiographic data presented in the current study are largely concordant with recent quantitative anatomic data.⁴ This information, in conjunction with previous anatomic data, may help improve preoperative planning, augment intraoperative visualization, and assist in postoperative assessment of lateral ankle repairs and reconstructions.

In recent years, significant work has been completed regarding surgical repairs and reconstructions of the lateral ligament complex.^{3,5,6,25,30} As anatomic based surgical procedures become more common, including repair augmentations, arthroscopic repairs, and allograft reconstructions,

improved multimodal intraoperative guidance will allow for accurate anatomic restoration.^{8,13,19,29,30} In the cases of arthroscopic repair, radiographic guidance would help compensate for any potentially lost anatomic landmarks apparent during open repair. Lateral and mortise radiographic reference data allow for more accurate placement of ATFL and CFL reconstruction tunnels intraoperatively and accurate postoperative evaluation of the placement of these reconstructions. Overall, radiographic data will augment current anatomic references and improve the anatomic accuracy of lateral ankle procedures.

In cases of lateral ankle instability requiring allograft reconstruction of the ATFL and CFL, anatomic placement of reconstruction tunnels should help to restore native joint kinematics and minimize graft elongation over time. In such indications, the 2-dimensional radiographic parameters defined in this study provide a methodology for verifying anatomic placement of guidepins, based on previously described 3-dimensional anatomic data prior to tunnel reaming. In a quantitative anatomy study, Clanton et al⁴ reported that the ATFL originated 13.8 mm (95% CI, 12.3-15.3) anterior and superior from the inferior tip of the lateral malleolus, 49.8% of the distance between the inferior tip of the lateral malleolus and the anterior fibular tubercle along the anterior fibular border, and inserted on

the talus 17.8 mm (95% CI, 16.3-19.3) anterior and superior from the apex of the lateral talar process. Radiographically, it was found that the ATFL originated 8.4 ± 1.8 mm anterior and superior to the inferior tip of the lateral malleolus, 35.7% \pm 8.9% of the absolute distance between the inferior tip of lateral malleolus and the anterior fibular tubercle, and inserted on the talus 13.8 ± 2.0 mm anterior and superior to the apex of the lateral talar process on the lateral view. Similarly, Clanton et al⁴ reported that the CFL attached on the fibula 5.3 mm (95% CI, 4.2-6.5) anterior and superior to the inferior tip of the lateral malleolus, 16.2% of the distance between the inferior tip of the lateral malleolus and the anterior fibular tubercle along the anterior fibular border, and 16.3 mm (95% CI, 14.5-18.1) posterior and superior to the posterior point of the peroneal tubercle on the calcaneus. On the lateral radiographic view in this study, the CFL attached 5.0 ± 1.4 mm anterior and superior to the inferior tip of the lateral malleolus, 21.1% \pm 6.4% of the absolute distance between the inferior tip of lateral malleolus and the anterior fibular tubercle, and attached on the calcaneus 18.5 ± 4.6 mm posterior and superior to the posterior point of the peroneal tubercle. These corresponding measurements and percentages are similar but not identical, which can be attributed to a combination of potentially contributing variables. Foremost, legitimate quantitative differences may exist because of anatomic variability and size and sex differences between specimen samples. After excluding 1 specimen, the present study included 11 specimens (9 male, 2 female) with mean height and foot length (\pm SD) of 174.1 ± 8.1 cm and 24.8 ± 1.8 cm, respectively. Second, the comparison assumes that the same osseous landmarks described by Clanton et al⁴ are readily apparent radiographically. Although the authors attempted to select radiographic landmarks coincident with those previously described, there may have been slight differences in the observation of radiographically visible and physically palpable landmarks and bony prominences. Furthermore, relative distance percentages in the present radiographic study were calculated using absolute straight-line distances because of limitations of the PACS measurement tools, while Clanton et al⁴ calculated percentages along the curved contour of the anterior fibular border. In addition, radiographic distances are inherently 2-dimensional and influenced by the rotation of the ankle for a given radiographic view, and therefore distances and percentages may not be directly comparable to the 3-dimensional anatomic data described by Clanton et al.⁴

Some limitations are acknowledged with respect to the findings of this study. Foremost, the sample size of the current study was relatively small; however, it is consistent with previous radiographic landmark studies.^{11,22,23,32} The included specimens were older than the population undergoing lateral ankle ligament repair/reconstruction; however, specimens were rigorously screened for osseous abnormalities and gross anatomic derangements. The authors also acknowledge a potential sex bias in the specimen sample with 9 male and 2 female specimens; however, because of the drilling required in this study, bone quality was a concern, hence the preferential selection of male specimens. Furthermore, no adequately powered

statistical comparison between sexes could be performed. The specimen samples had a mean height and foot length (\pm SD) of 174.1 ± 8.1 cm and 24.8 ± 1.8 cm, respectively, which is approximately equivalent to the average height for American men 20 years and older according to the National Health Statistics report.¹⁶ Although this somewhat limits the direct application of the defined radiographic data to smaller female individuals, the authors believe that the data accurately characterize the population of interest. Hootman et al¹⁰ demonstrated that the greatest incidence and frequency of athletic ankle sprains in National Collegiate Athletic Association (NCAA) athletics occur in men's football and basketball. Furthermore, lateral ankle ligament reconstruction, a procedure for which the application of the data presented is intended, would most likely be clinically indicated for larger patients who place significantly more strain on the lateral ligament structures. In this respect, the radiographic data presented would also be directly applicable to this patient population.

Furthermore, based on the relative uniformity in the data (as indicated by the standard deviation) and congruency with previous anatomic data, the authors are confident in the radiographic anatomic relationships defined in this study. However, the authors do not intend for these data to supersede or replace current surgical references but rather augment current surgical navigation. Intraoperatively, the combination of additional anatomic references and surgeon experience will dictate adjustments in reconstruction tunnel placement within the ranges defined by radiographic parameters. Finally, the present study reports 2-dimensional distances representative of 3-dimensional relationships; therefore, these distances are subject to variability with orientation of the radiographic view and must be interpreted accordingly. To reduce the risk of iatrogenic soft tissue injury, recommendations based on these data must be implemented in conjunction with additional anatomic data describing the intervening soft tissues not seen radiographically.

CONCLUSION

In this laboratory study, radiographic guidelines quantifying the anatomic origins and insertions of the lateral ankle ligaments were defined. The objective radiographic guidelines established by this study will assist in preoperative planning, improve intraoperative assessment, and supplement postoperative evaluation of lateral ankle repairs and reconstructions.

ACKNOWLEDGMENT

The authors acknowledge Grant Dornan, MSc, for his statistical expertise and Kelly Adair for assistance with surgical expertise and study material acquisition.

REFERENCES

1. Bennett WF. Lateral ankle sprains, part I: anatomy, biomechanics, diagnosis, and natural history. *Orthop Rev.* 1994;23(5):381-387.

2. Burks RT, Morgan J. Anatomy of the lateral ankle ligaments. *Am J Sports Med.* 1994;22(1):72-77.
3. Clanton TO. Failed lateral ankle ligament reconstruction. In: Nunley JA, Pfeffer GB, Sanders RW, Trepman E, eds. *Advanced Reconstruction Foot and Ankle.* Rosemont, IL: American Academy of Orthopaedic Surgeons; 2004;267-272.
4. Clanton TO, Campbell KJ, Wilson KJ, et al. Qualitative and quantitative anatomic investigation of the lateral ankle ligaments for surgical reconstruction procedures. *J Bone Joint Surg Am.* 2014;96(12):e98.
5. Clanton TO, Viens NA, Campbell KJ, LaPrade RF, Wijdicks CA. Anterior talofibular ligament ruptures, part 1: biomechanical comparison of augmented Brostrom repair techniques with the intact anterior talofibular ligament. *Am J Sports Med.* 2013;34:587-592.
6. Coughlin MJ, Schenck RC Jr, Grebing BR, Treme G. Comprehensive reconstruction of the lateral ankle for chronic instability using a free gracilis graft. *Foot Ankle Int.* 2004;25:231-241.
7. Garrick JG. The frequency of injury, mechanism of injury, and epidemiology of ankle sprains. *Am J Sports Med.* 1977;5(6):241-242.
8. Giza E, Shin EC, Wong SE, et al. Arthroscopic suture anchor repair of the lateral ligament ankle complex: a cadaveric study. *Am J Sports Med.* 2013;41(11):2567-2572.
9. Golano P, Vega J, de Leeuw PAJ, et al. Anatomy of the ankle ligaments: a pictorial essay. *Knee Surg Sports Traumatol Arthrosc.* 2010;18(5):557-569.
10. Hootman JM, Dick R, Agel J. Epidemiology of collegiate injuries for 15 sports: summary and recommendations for injury prevention initiatives. *J Athl Train.* 2007;42(2):311-319.
11. Johansson AM, Anderson CJ, Wijdicks CA, Engebretsen L, LaPrade RF. Radiographic landmarks for tunnel positioning in posterior cruciate ligament reconstructions. *Am J Sports Med.* 2013;41(1):35-42.
12. Junge A, Engebretsen L, Mountjoy ML, et al. Sports injuries during the summer Olympic games 2008. *Am J Sports Med.* 2009;37(11):2165-2172.
13. Kim ES, Lee KT, Park JS, Lee YK. Arthroscopic anterior talofibular ligament repair for chronic ankle instability with a suture anchor technique. *Orthopedics.* 2011;34(4). doi: 10.3928/01477447-20110228-03.
14. Konradsen L, Bech L, Ehrenbjerg M, Nickelsen T. Seven years follow-up after ankle inversion trauma. *Scand J Med Sci Sports.* 2002;12(3):129-135.
15. Malliaropoulos N, Ntessalen M, Papacostas E, Longo UG, Maffulli N. Reinjury after acute lateral ankle sprains in elite track and field athletes. *Am J Sports Med.* 2009;37(9):1755-1761.
16. McDowell MA, Fryar CD, Ogden CL, Flegal KM. *Anthropometric Reference Data for Children and Adults: United States, 2003-2006.* National Health Statistics Reports; no 10. Hyattsville, MD: National Center for Health Statistics; 2008.
17. Milner CE, Soames RW. Anatomy of the collateral ligaments of the human ankle joint. *Foot Ankle Int.* 1998;19(11):757-760.
18. Montagne J, Chevrot A, Galmiche JM, Chafetz N, eds. *Atlas of Foot Radiology.* New York, NY: Mason Publishing; 1983.
19. Nery C, Raduan F, Del Buono A, Asaumi ID, Cohen M, Maffulli N. Arthroscopic assisted Brostrom-Gould for chronic ankle instability: a long-term follow-up. *Am J Sports Med.* 2011;39(11):2381-2388.
20. Neuschwander TB, Indresano AA, Hughes TH, Smith BW. Footprint of the lateral ligament complex of the ankle. *Foot Ankle Int.* 2013;34(4):582-586.
21. Petersen W, Rembitzki IV, Keppenburg AG, et al. Treatment of acute ankle ligament injuries: a systematic review. *Arch Orthop Trauma Surg.* 2013;133(8):1129-1141.
22. Pietrini SD, LaPrade RF, Griffith CJ, Wijdicks CA, Ziegler CG. Radiographic identification of the primary posterolateral knee structures. *Am J Sports Med.* 2009;37(3):542-551.
23. Pietrini SD, Ziegler CG, Anderson CJ, et al. Radiographic landmarks for tunnel positioning in double-bundle ACL reconstructions. *Knee Surg Sports Traumatol Arthrosc.* 2011;19(5):792-800.
24. Raheem OA, O'Brien M. Anatomical review of the lateral collateral ligaments of the ankle: a cadaveric study. *Anat Sci Int.* 2011;86(4):189-193.
25. Schenck RC Jr, Coughlin MJ. Lateral ankle instability and revision surgery alternatives in the athlete. *Foot Ankle Clin North Am.* 2009;14:205-214.
26. Shrout PE, Fleiss JL. Intraclass correlations: uses in assessing rater reliability. *Psychol Bull.* 1979;86:420-428.
27. Taser F, Shafiq Q, Ebraheim NA. Anatomy of lateral ankle ligaments and their relationship to bony landmarks. *Surg Radiol Anat.* 2006;28(4):391-397.
28. van den Bekerom MP, Oostra RJ, Alvarez PG, van Dijk CN. The anatomy in relation to injury of the lateral collateral ligaments of the ankle: a current concepts review. *Clin Anat.* 2008;21(7):619-626.
29. Viens NA, Wijdicks CA, Campbell KJ, LaPrade RF, Clanton TO. Anterior talofibular ligament rupture, part 1: Biomechanical comparison of augmented Brostrom repair techniques to the intact anterior talofibular ligament. *Am J Sports Med.* 2014;42(2):405-411.
30. Waldrop NE III, Wijdicks CA, Jansson KS, LaPrade RF, Clanton TO. Anatomic suture anchor versus the Brostrom technique for anterior talofibular ligament repair: a biomechanical comparison. *Am J Sports Med.* 2012;40(11):2590-2596.
31. Waterman BR, Owens BD, Davey S, Zacchilli MA, Belmont PJ. Epidemiology of ankle sprains in the United States. *J Bone Joint Surg Am.* 2010;92(13):2279-2284.
32. Wijdicks CA, Griffith CJ, LaPrade RF, et al. Radiographic identification of the primary medial knee structures. *J Bone Joint Surg Am.* 2009;91(3):521-529.
33. Yildiz S, Yalcin B. The anterior talofibular and calcaneofibular ligaments: an anatomic study. *Surg Radiol Anat.* 2013;35(6):511-516.

For reprints and permission queries, please visit SAGE's Web site at <http://www.sagepub.com/journalsPermissions.nav>